View Online / Journal Homepage / Table of Contents for this issue

PCCP

Time dependent wave packet study of the electronically non-adiabatic $Cl + H_2$ reaction using a one-dimensional model

Frederico V. Prudente,[a] Antonio Riganelli[b] and Jorge M. C. Marques[c]

[a] *Instituto de Física, Universidade Federal da Bahia, 40210-340, Salvador, BA, Brazil. E-mail: prudente@ufba.br*
[b] *Dipartimento di Chimica, Universitá di Perugia, 06123 Perugia, Italy. E-mail: auto@impact.dyn.unipg.it*
[c] *Departamento de Química, Universidade de Coimbra, 3004-355 Coimbra, Portugal. E-mail: qtmarque@ci.uc.pt*

Received 24th January 2003, Accepted 3rd April 2003
First published as an Advance Article on the web 22nd April 2003

Downloaded on 15 December 2011
Published on 22 April 2003 on http://pubs.rsc.org | doi:10.1039/B301010D

We report a time dependent wave packet calculation of the electronically non-adiabatic $Cl + H_2$ reaction using a one-dimensional diabatic potential model. The funnel resonances are characterized for a large range of the energy, and the results compared with recent time independent calculations using the same model.

Introduction

Non-adiabatic effects are known to play a fundamental role in the dynamics of many chemical processes, *e.g.*, photodissociation, predissociation, electronic quenching, charge transfer, and spin-changing reactions (see refs. 1–4 and references therein). Moreover, quantum mechanical resonances can appear in both full and half-scattering processes involving more than one electronic state.[5,6] Thus, the analysis and characterization of such quasi-bound states (that clearly arise in the pattern of cross sections) becomes crucial to understand the relevant dynamics of the particular system. Due to the unequivocal quantum nature of these phenomena, it is of major importance the development of efficient numerical procedures based on quantum mechanics to treat systems where two or more (diabatic or adiabatic) potential energy surfaces are involved.

A reliable and efficient method which has been used for treating molecular collision processes within the Born–Oppenheimer or adiabatic framework is the time dependent wave packet propagation (see ref. 7 and references therein). This methodology presents several advantages over the time independent one (see ref. 7 for a detailed discussion). These are expected to be also observed in the study of the non-adiabatic reactions using either diabatic and adiabatic representations.[8] Moreover, the time dependent wave packet technique allows a straightforward treatment of collision-induced dissociation.[9] However, a detailed analysis of resonances due to the non-adiabatic coupling (*e.g.*, calculation of energies and widths of such resonance states) is not very common in time dependent wave packet studies,[10] although their effects have been observed in many of such investigations.[11–16] An explanation for this is that in the presence of long-lived resonance states such a method needs, in principle, longer propagation times.

On the other hand, the determination of resonance states in adiabatic processes by using time dependent wave packet methods have been studied by several authors (see, *e.g.*, refs. 17–24). In general, several methods have been proposed to avoid a long propagation time. Examples are the Prony method[25] as used by Gray[18] and the hybrid approach which uses the filter diagonalization method for the calculation of resonances.[21,23,26] In these procedures, the initial wave packet is propagated up to some time at which direct scattering is complete, and then the resonance calculation is performed to extrapolate long-time behavior of the wave packet or its correlation function. They are particularly interesting to treat larger systems for which long propagation times become out of reach from a computational point of view. However, it is important to point out that the time dependent calculations by using long time propagation are of interest when it is possible to be done,[27] because they can provide the "exact" time dependent results in a numerical sense.

The major goal of this paper stems on showing the capacity of a wave packet procedure to obtain detailed and accurate information about narrow resonances from the scattering information by using a long-time propagation. In particular, this study presents the first detailed comparison between time dependent and time independent quantum calculations of the resonances arising in the non-adiabatic dynamics of the $Cl + H_2$ reaction, which plays a very important role in atmospheric chemistry. Because of this, the title system has been extensively studied both experimentally and theoretically (see, *e.g.*,ref. 28 and references therein). In order to compare our results with those by Friedman *et al.*[29,30] obtained within the time independent framework, we have used the same one-dimensional diabatic two-state potential model for $Cl + H_2$. Indeed, the model has been shown to have several isolated narrow resonances associated with states trapped in the upper adiabatic potential curve.[29,30] In turn, we characterize 24 of such resonances by calculating the corresponding energies and widths, and also present accurate results for transition probabilities, delay time matrix elements, and lifetime matrix as a function of the energy.

The paper is organized as follows. In the next section we briefly describe the time dependent wave packet methodology employed here to study the resonance states (eigenenergies and widths), and other typical scattering results. In section 3, we give the details of the wave-packet propagations, and present the results as well as a comparison with time-independent calculations. Conclusions are gathered in section 4.

This journal is © The Owner Societies 2003

View Online

Published on 22 April 2003 on http://pubs.rsc.org | doi:10.1039/B301010D
Downloaded on 15 December 2011

2. Methodology

The dynamics of the title system has been studied by using the one-dimensional time dependent Schrödinger equation in a diabatic representation, *i.e.*,

$$i\hbar\frac{\partial \boldsymbol{\Psi}}{\partial t} = -\frac{\hbar^2}{2\mu}\frac{d^2\boldsymbol{\Psi}}{dx^2} + \hat{V}\boldsymbol{\Psi} \quad (1)$$

where $\hat{V}$ is the 2×2 diabatic potential energy matrix given by

$$\hat{V} = \begin{pmatrix} V_{11} & V_{12} \\ V_{12} & V_{22} \end{pmatrix} \quad (2)$$

μ is the reduced mass of the $^{35}Cl + H_2$ system, and $\boldsymbol{\Psi}$ is the diabatic wave function vector given by

$$\boldsymbol{\Psi} = \begin{pmatrix} \psi_1(x;t) \\ \psi_2(x;t) \end{pmatrix} \quad (3)$$

The solution of eqn. (1) can be written formally as

$$\boldsymbol{\Psi}(x;t) = \exp\left(-\frac{i}{\hbar}\hat{H}\right)\boldsymbol{\Psi}(x;0) \quad (4)$$

where $\hat{H}$ is the $1D$ two-state diabatic Hamiltonian operator as given in eqn. (1) and $\boldsymbol{\Psi}(x;0)$ is the initial wave packet vector, which has been represented on a equally spaced grid in coordinate space. The fast Fourier transform algorithm[31,32] has been used to evaluate the action of the kinetic energy operator on the wave functions ψ_1 and ψ_2, while the short-time iterative Lanczos method[33,34] has been applied to propagate the initial wave packet vector $\boldsymbol{\Psi}(x;0)$ over the two coupled potential energy curves. The two components of the initial wave packet vector are composed by a normalized Gaussian function with the form

$$\psi_{[1,2]}(x;0) = \left(\frac{1}{2\pi\sigma^2}\right)^{1/4}\exp\left[-\beta(x-x_0)^2\right] \times \exp[ip_0(x-x_0)] \quad (5)$$

and $\psi_{[2,1]}(x;0) = 0$, depending whether the wave packet is propagated initially from the right to the left as shown in Fig. 1 or *vice-versa*. The usual Gaussian parameters σ, $\beta = 1/(4\sigma^2)$, p_0, and x_0 are assigned prior to calculation. The parameters x_0 and p_0 represent the initial wave packet position and initial wave packet momentum, respectively.

Since the diabatic wave function is expected to be trapped in the V_{11} funnel during a long time, we have then multiplied the wave packet vector by a damping function[35]

$$F(x) = \sin\left[\frac{\pi}{2}\frac{(X_{mask} + \Delta X_{mask} - x)}{\Delta X_{mask}}\right], \quad x \geq X_{mask} \quad (6)$$

at each time step to absorb its scattered parts before it reaches the boundaries of the grid resulting in a $\sin^2$ masking. In eqn. (6), X_{mask} represents the point at which the masking function is initiated and $\Delta X_{mask} = X_{max}–X_{mask}$ is the width over which the function decays. This method of damping is equivalent to add a negative imaginary potential (NIP) to the real potential.[17,36] Particularly for systems with many isolated and narrow resonances, its use seems to be more appropriate[35] than the NIP method.

In the energy range of interest only two asymptotic channels are open: (i) propagation of ψ_1 to $x \to +\infty$ over V_{11}, and (ii) propagation of ψ_2 to $x \to -\infty$ over V_{22}. Thus, the scattering matrix (S-matrix) is a 2×2 symmetric, unitary matrix whose diagonal elements (S_{11} and S_{22}) correspond to reflection amplitudes while the off-diagonal S_{12} and S_{21} are the transmission ones. The elements S_{mn} ($m,n = 1,2$) may be calculated as

$$S_{mn}(E) = \frac{\sqrt{|k_n k_m|}\exp(ik_n x_n)}{2\pi\mu g(k_m)}\int \psi_n(x_n;t)\exp\left(\frac{iEt}{\hbar}\right)dt \quad (7)$$

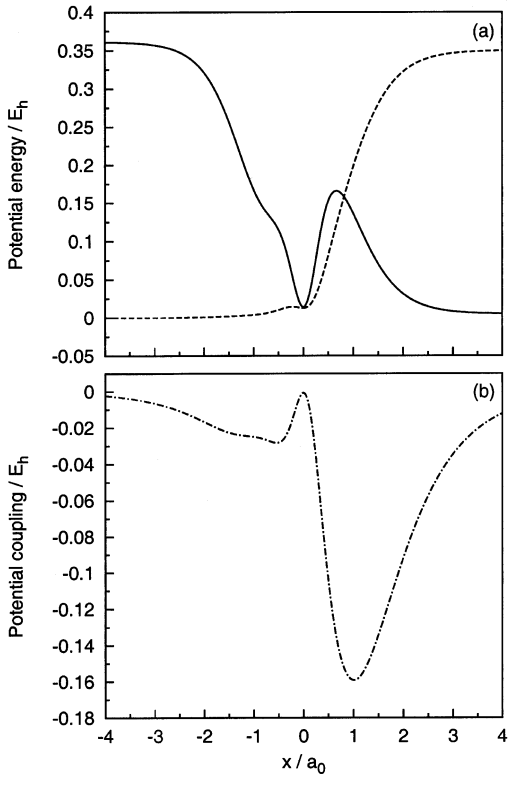

Fig. 1 One-dimensional diabatic potential model for the $Cl + H_2$ reaction: (a) V_{11} (full line) and V_{22} (dashed line) potential energy curves; (b) V_{12} coupling function. See ref. 29 for details.

where E is the total energy of the system, $k_1 = -\sqrt{2\mu[E - V_{11}(x_1)]}$, $k_2 = \sqrt{2\mu[E - V_{22}(x_2)]}$, the function g is the Fourier transform of the non-zero initial wave packet component $\psi_{[1,2]}(x,0)$ which is given by

$$g(k) = \frac{\sqrt{2\sigma}}{(2\pi)^{1/4}}\exp\left[-\sigma^2(k-p_0)^2\right]\exp(-ix_0k) \quad (8)$$

and x_1 [x_2] is some fixed asymptotically large distance at channel 1 [2].

Finally, the resonances may be characterized by the lifetime matrix $\boldsymbol{Q}$ and the delay-time matrix $\Delta\boldsymbol{t}$, whose elements are given through the expressions:[37,38]

$$Q_{nm} = i\hbar\sum_{l=1}^{2} S_{nl}(dS_{ml}{}^*/dE) \quad (9)$$

$$\Delta t_{nm} = \mathrm{Im}[\hbar(S_{mn})^{-1}dS_{mn}/dE] \quad (m,n = 1,2) \quad (10)$$

where $S_{ml}{}^*$ denotes the complex conjugate of the scattering matrix element S_{ml}. In addition, it is important to point out that, close to each resonance α, the largest eigenvalue of the $\boldsymbol{Q}$ matrix, q_{11}, which represents the longest lifetime of the incident particle,[37,38] has a Lorentzian form given by[39]

Table 1 Local maxima in the trace of $\boldsymbol{Q}$ at energies E_{max} and the eigenvalues of Q at energies E_{max}. Second entry for each state refers to the results of ref. 29

α	E_{max}/E_h	Tr($\boldsymbol{Q}$)/fs	q_{11}/fs	q_{22}/fs
0	0.027975	1100.14	1098.92	1.216
	0.027974	1100.07	1098.86	1.217
1	0.053911	835.51	835.14	0.376
	0.053911	835.51	835.13	0.377

Table 2 Local maxima in the delay times Δt_{nm} at energies E^{nm}_{max}. Second entry for each state refers to the results of ref. 29

α	E^{11}_{max}/E_h	Δt_{11}/fs	E^{12}_{max}/E_h	Δt_{12}/fs	E^{22}_{max}/E_h	Δt_{22}/fs
0	0.027975	549.38	0.027977	549.01	0.027975	550.77
	0.027974	549.24	0.027974	549.94	0.027974	550.64
1	0.053911	418.02	0.053911	417.63	0.053911	417.50
	0.053911	417.97	0.053911	417.71	0.053911	417.52

$$q_{11}(E) = \Gamma_\alpha/[(E - E_\alpha)^2 + (\Gamma_\alpha/2)^2] \quad (11)$$

where E_α and Γ_α are, respectively, the energy and width of resonance α. Once the $\boldsymbol{Q}$ matrix is calculated by eqn. (9), it is possible to obtain E_α and Γ_α through a least-squares fit using eqn. (11).

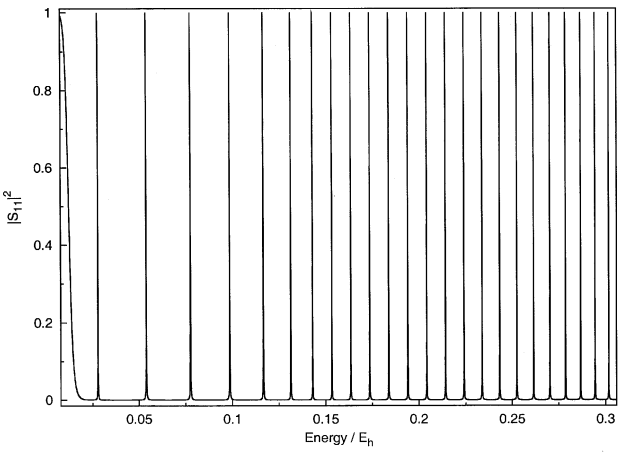

Fig. 3 Reflection probability $|S_{11}|^2$ as a function of scattering energy.

3. Results and comparison

We have carried out a detailed study of the electronically non-adiabatic $Cl + H_2$ reaction on a one-dimensional model by solving the time dependent Schrödinger equation in a diabatic representation [eqn. (1)]. In turn, we have calculated the S-matrix, transition probabilities, delay-time matrix elements, and lifetime matrix as a function of the energy, in order to characterize the funnel resonances of the title system. Friedman *et al.*[29] have proposed one-dimensional potential energy functions (V_{11} and V_{22}) and non-adiabatic coupling term (V_{12}) that models the collinear minimum energy path of the three-dimensional ClH_2 surfaces. In order to compare our results with their time-independent ones,[29,30] we have used the same potential energy curves that were adopted in ref. 30 (case V of ref. 29). In particular, the diabatic $V_{11}(x)$ and $V_{22}(x)$ potential curves and the corresponding coupling $V_{12}(x)$ term are shown in panel (a) and panel (b) of Fig. 1; x represents the reaction coordinate. The analytical expressions and the numerical parameters for V_{11}, V_{12} and V_{22} are presented in ref. 29 [eqns. (32)–(36) and Tables 1 and 2] and in ref. 30 [eqns. (30)–(34) and Table 1]. These functions may be combined to obtain the corresponding adiabatic potential energy curves whose ground state is similar to $Cl + H_2$ surface

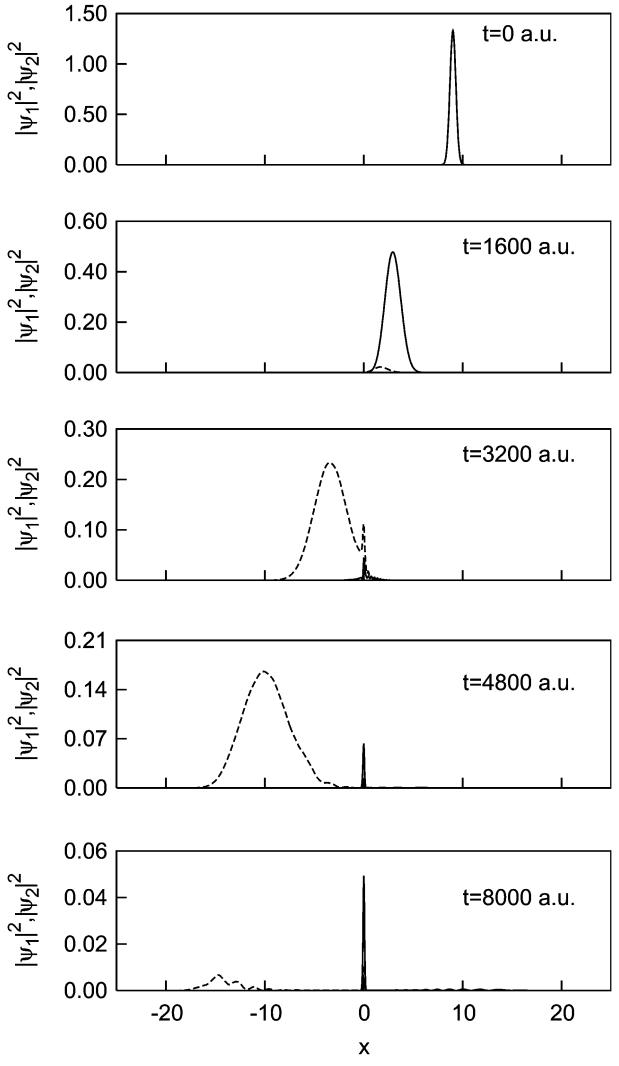

Fig. 2 Snapshots of the time evolution of the $|\psi_1(x,t)|^2$ (full line) and $|\psi_2(x,t)|^2$ (dashed line) wave packet components.

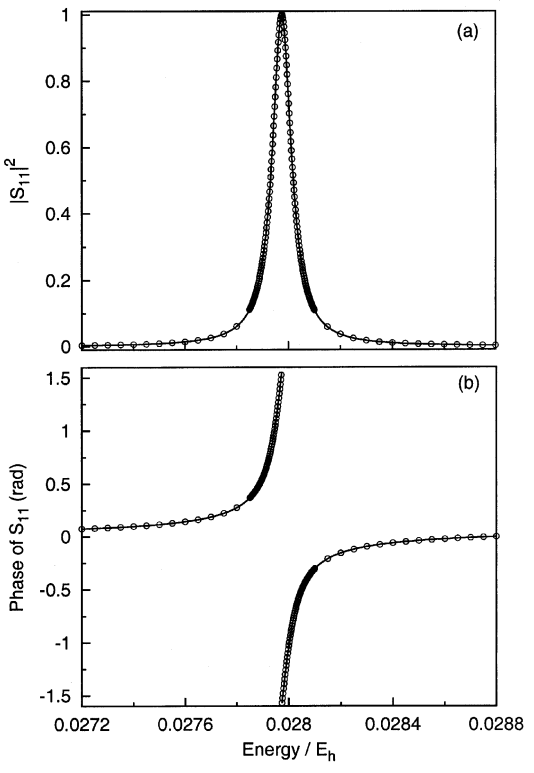

Fig. 4 Diagonal S-matrix elements in the vicinity of the $\alpha = 0$ resonance position: (a) magnitude and (b) phase of S_{11}. The solid line is the result of this work and the circles represent the results from ref. 29.

Published on 22 April 2003 on http://pubs.rsc.org | doi:10.1039/B301010D
Downloaded on 15 December 2011

View Online

Published on 22 April 2003 on http://pubs.rsc.org | doi:10.1039/B301010D
Downloaded on 15 December 2011

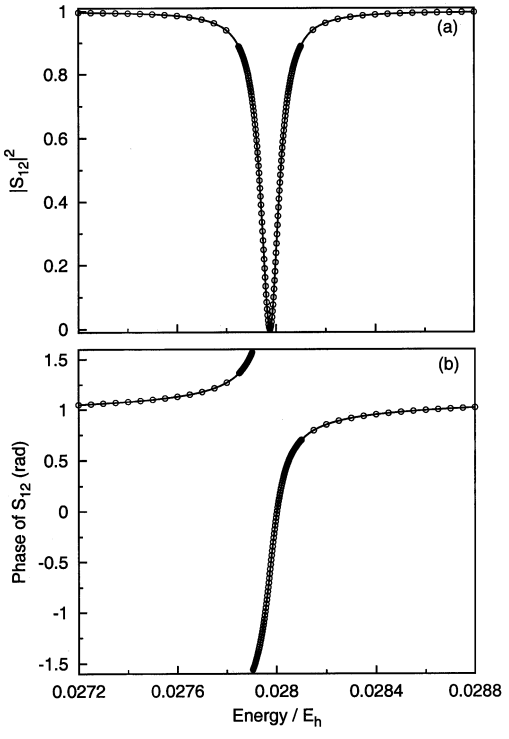

Fig. 5 Off-diagonal S-matrix elements in the vicinity of the $\alpha = 0$ resonance position: (a) magnitude and (b) phase of S_{12}. The solid line is the present result and the circles represent the results from ref. 29.

of ref. 5 and the excited state has a minimum (exciplex funnel) over the saddle point located at $x = 0\ a_0$.[29,30]

The energy range considered in present work is $0.007 < E/E_h < 0.302$, where the first 24 funnel resonances may be found for the title system. To obtain the results shown here, five wave packet propagations have been performed for different values of p_0. These are obtained from an initial energy E, once $p_0 = \sqrt{2\mu(E - V_{11}(x_1))}$ or $p_0 = -\sqrt{2\mu(E - V_{22}(x_2))}$, depending on whether the initial wave packet is localized at channel 1 ($x_0 > 0$) or channel 2 ($x_0 < 0$). In turn, the five values of energy used are: (I) $0.03E_h$; (II) $0.08E_h$; (III) $0.14E_h$; (IV) $0.21E_h$; (V) $0.29E_h$. In each case, a grid with 2048 equally-spaced points extending from $x = -45\ a_0$ to $x = 45\ a_0$ has been used to represent the wave functions. Moreover, we have assigned $\sigma = 0.3$ and $x_0 = \pm 9.0$ (all in au), while the propagation has been taken always during 40 000 time steps of 8 au each; the reduced mass of the $^{35}Cl + H_2$ is 3474.057 m_e. An example of the time evolution of the $\psi_{[1,2]}(x,t)$ wave packet components is displayed in Fig. 2.

The main results are shown in Figs. 3–7 and Tables 1–3. The calculated reflexion probability $P_{11} = |S_{11}|^2$ as a function of energy is displayed in Fig. 3, where we can locate 24 funnel resonances (labeled $\alpha = 0,\cdots,23$). In Figs. 4 and 5 we have compared our results for diagonal (S_{11}) and off-diagonal (S_{12}) elements from eqn. (7) with an accurate time independent scattering calculation[29] in the vicinity of the first resonance. It can be observed that the agreement is excellent for both the magnitude and the phase of the S_{11} and S_{12} elements (the relative errors between our results and the time independent ones shown in Figs. 4 and 5 are lesser than 10^{-4}). In order to follow the detailed comparison with the quantum time independent

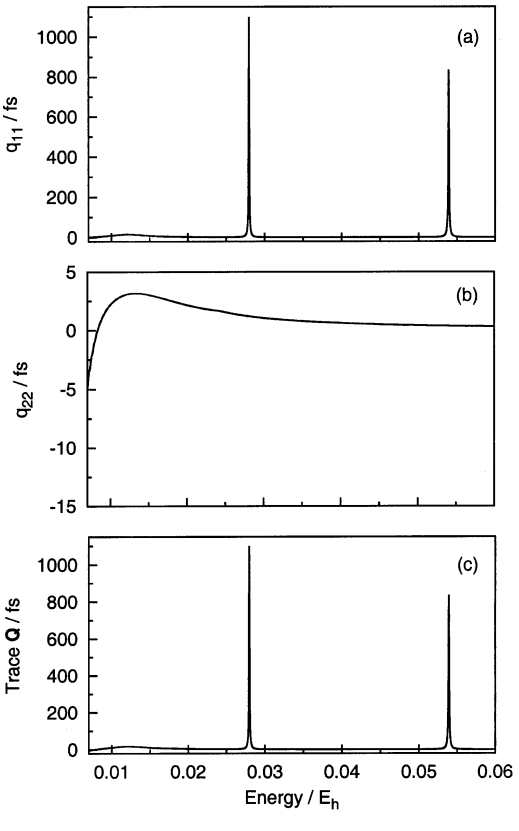

Fig. 6 Eigenvalues and trace of the lifetime matrix $\boldsymbol{Q}$ as a function of scattering energy for $\alpha = 0$ and $\alpha = 1$ resonances: (a) q_{11}; (b) q_{22}; and (c) trace of $\boldsymbol{Q}$. Full lines represent the results of this work, while those from ref. 29 are shown by the dashed lines (they are indistinguishable here because both results are essentially identical).

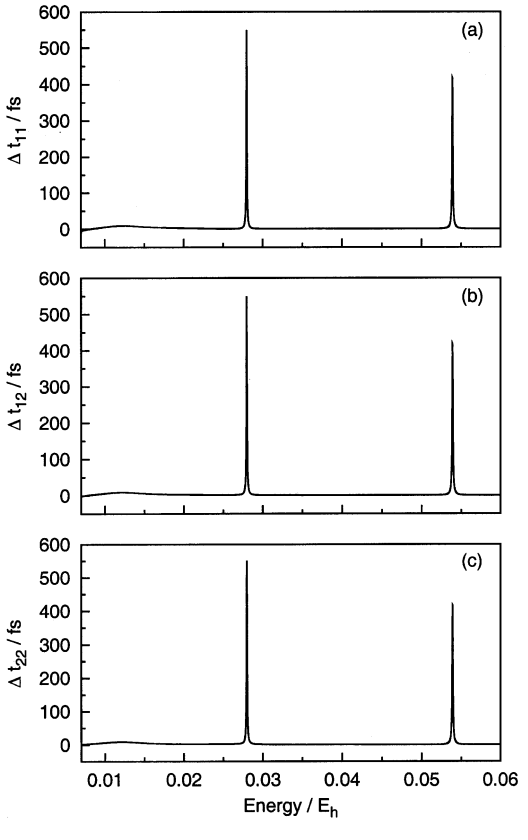

Fig. 7 Delay time matrix elements Δt_{nm} as a function of scattering energy for $\alpha = 0$ and $\alpha = 1$ resonances: (a) Δt_{11}; (b) Δt_{22}; (c) Δt_{12}. Full lines represent the results of this work, while those from ref. 29 are shown by the dashed lines (they are indistinguishable here because both results are essentially identical).

View Online

Table 3 Eigenenergies and widths for the funnel resonances

	Present results			Results from ref. 30	
α	Run[a]	E_α/E_h	Γ/E_h	E_α/E_h	Γ/E_h
0	I	0.027 975 416 78	0.000 088 138 26	0.027 975 417 22	0.000 088 137 56
1	I	0.053 911 770 82	0.000 115 906 89	0.053 911 771 56	0.000 115 906 98
2	II	0.077 517 487 55	0.000 122 313 28	0.077 517 488 75	0.000 122 313 36
3	II	0.098 569 074 69	0.000 118 387 17	0.098 569 076 08	0.000 118 387 28
4	II	0.116 695 168 7	0.000 106 040 4	0.116 695 169 8	0.000 106 040 6
5	II	0.131 428 293 4	0.000 087 232 9	0.131 428 294 2	0.000 087 232 6
6	III	0.143 025 073 1	0.000 073 525 9	0.143 025 074 5	0.000 073 525 9
7	III	0.153 312 020 0	0.000 072 404 2	0.153 312 022 0	0.000 072 404 2
8	III	0.163 483 672 9	0.000 074 266 4	0.163 483 675 4	0.000 074 266 4
9	III	0.173 686 828 2	0.000 076 159 2	0.173 686 831 4	0.000 076 159 2
10	III	0.183 905 231 2	0.000 077 728 8	0.183 905 235 0	0.000 077 728 7
11	IV	0.194 099 023 2	0.000 078 902 2	0.194 099 027 5	0.000 078 902 3
12	IV	0.204 226 412 7	0.000 079 671 1	0.204 226 417 7	0.000 079 671 2
13	IV	0.214 247 956 0	0.000 080 043 7	0.214 247 961 5	0.000 080 043 7
14	IV	0.224 127 294 5	0.000 080 032 5	0.224 127 300 3	0.000 080 032 5
15	IV	0.233 830 978 5	0.000 079 650 5	0.233 830 984 6	0.000 079 650 5
16	IV	0.243 328 084 4	0.000 078 910 3	0.243 328 090 8	0.000 078 910 3
17	IV	0.252 589 822 5	0.000 077 823 4	0.252 589 829 2	0.000 077 823 4
18	V	0.261 589 186 6	0.000 076 400 5	0.261 589 193 7	0.000 076 400 4
19	V	0.270 300 653 2	0.000 074 651 1	0.270 300 660 4	0.000 074 651 1
20	V	0.278 699 921 5	0.000 072 584 2	0.278 699 929 0	0.000 072 584 4
21	V	0.286 763 690 1	0.000 070 208 1	0.286 763 697 3	0.000 070 208 5
22	V	0.294 469 450 3	0.000 067 530 2	0.294 469 457 1	0.000 067 530 6
23	V	0.301 795 291 6	0.000 064 556 7	0.301 795 299 5	0.000 064 556 8

[a] Each run represents the time dependent wave packet calculation for a particular initial energy E parameter: I) $E = 0.03E_h$; II) $E = 0.08E_h$; III) $E = 0.14E_h$; IV) $E = 0.21E_h$; and V) $E = 0.29E_h$.

Published on 22 April 2003 on http://pubs.rsc.org | doi:10.1039/B301010D
Downloaded on 15 December 2011

results,[29,30] Fig. 6 shows the ***Q***-matrix for the first two funnel resonances, while Fig. 7 represents the corresponding delay-time matrix elements. Clearly, it is patent the good agreement, in all cases, between the present time dependent results and those obtained by Friedman and coworkers.[29] Moreover, the local maxima arising in the trace of the ***Q***-matrix and the corresponding eigenvalues, and the delay-time matrix elements for $\alpha = 0$ and $\alpha = 1$ are characterized in Tables 1 and 2, respectively. Once again the time dependent results are in good agreement with the time independent ones.[29] In addition, these results constitute an indication of isolated, narrow resonances associated with long-lived metastable states.

The individual values of energies and widths for all 24 resonances have been determined from a least-squares fit of eqn. (11). For the fit we have used the Powell's direction set method,[40] where we add a background constant in eqn. (11) to take into account the effects of far away resonances. These energies and widths are presented in Table 3 and compared with those of Friedman and coworkers[30] which were calculated using the time independent complex coordinate method. Particularly interesting is that our calculation can mimic their resonance energies within, at least, 7 significant figures; also the Γ-values of the widths present good agreement (within, at least, 4 significant figures) with the results of ref. 30. This is especially relevant because it shows that the time dependent procedures are able to characterize funnel resonances within a great accuracy. It is important to point out that all our values in Table 3 are obtained from only five sets of calculations (labeled by I, II, III, IV, and V, corresponding to different energies as described above).

4. Conclusion remarks

The importance of metastable funnel resonances in the dynamics of the $Cl + H_2$ reaction has been investigated using a time dependent wave packet calculation and a one-dimensional non-adiabatic model. The results are in good agreement with those of Friedman *et al.*[29,30] using two different time-independent methodologies. In summary, this work clearly shows that wave packet calculations using a Lanczos method for the long time propagation is extremely accurate to study non-adiabatic dynamics of systems involving isolated, narrow resonances. Although we have not carried out a direct comparison on the performance between the present time-dependent method and the time-independent ones used by Friedman *et al.*[29,30] (which is out of the scope of this work), time-dependent wave packet calculations are, in general, less demanding in terms of computational effort. Moreover, it is also possible to use one of the hybrid methods cited in the Introduction, which avoids long propagation times, when these are not feasible. Thus, we believe that our methodology can be competitive when extended to fully dimensional non-adiabatic treatments. For instance, the work concerning the implementation of a computational code to treat quantum scattering processes with more dimensions involving two or more coupled potential energy surfaces is currently in progress and we expect to publish the first results elsewhere.

Acknowledgements

We are grateful to Ronald S. Friedman for providing us with all of the data from his time independent calculations (refs. 29 and 30).

References

1 J. C. Tully, in *Modern Theoretical Chemistry: Dynamics of Molecular Collisions*, ed. W. H. Miller, Plenum Press, New York, 1986, p. 217.
2 M. Baer, in *Theory of Chemical Reaction Dynamics*, ed. M. Baer, CRC, Boca Raton, FL, 1985, part II, p. 219.

View Online

3 H. Nakamura, *Int. Rev. Phys. Chem.*, 1991, **10**, 123.
4 D. R. Yarkony, *J. Phys. Chem.*, 1996, **100**, 18 612.
5 T. C. Allison, S. L. Mielke, D. W. Schwenke and D. G. Truhlar, *J. Chem. Soc., Faraday Trans.*, 1997, **93**, 825.
6 R. S. Friedman, I. Podzielinski, L. S. Cederbaum, V. M. Rayboy and N. Moiseyev, *J. Phys. Chem. A*, 2002, **106**, 4320.
7 N. Balakrishnan, C. Kalyanaraman and N. Sathyamurhy, *Phys. Rep.*, 1997, **280**, 79.
8 G. Parlant and D. R. Yarkony, *Int. J. Quantum Chem.: Quantum Chem. Symp.*, 1992, **26**, 737.
9 C. Leforestier, *Chem. Phys.*, 1984, **87**, 241.
10 L. M. Andersson, F. Burmeister, H. O. Karlsson and O. Goscinki, *Phys. Rev. A*, 2001, **65**, 12 705.
11 U. Manthe, H. Köppel and L. S. Cederbaum, *J. Chem. Phys.*, 1991, **95**, 1708.
12 B. Heumann, K. Weide, R. Düren and R. Schinke, *J. Chem. Phys.*, 1993, **98**, 5508.
13 G. Kroes, M. C. van Hemert, G. D. Billing and D. Neuhauser, *Chem. Phys. Lett.*, 1997, **271**, 311.
14 G. Kroes, M. C. van Hemert, G. D. Billing and D. Neuhauser, *J. Chem. Phys.*, 1997, **107**, 5757.
15 D. Simah, B. Hartke and H. Werner, *J. Chem. Phys.*, 1999, **111**, 4523.
16 A. N. Hussain and G. Roberts, *J. Chem. Phys.*, 1999, **110**, 2474.
17 R. H. Bisseling, R. Kosloff and J. Manz, *J. Chem. Phys*, 1985, **83**, 993.
18 S. K. Gray, *J. Chem. Phys.*, 1992, **96**, 6543.
19 R. Sadeghi and R. T. Skodje, *J. Chem. Phys.*, 1995, **102**, 193.
20 J. Dai and J. Z. H. Zhang, *J. Chem. Phys.*, 1996, **104**, 3664.
21 G. Kroes, M. R. Wall, J. W. Pang and D. Neuhauser, *J. Chem. Phys.*, 1997, **106**, 1800.
22 P. J. Krause and D. C. Clary, *Chem. Phys. Lett.*, 1997, **271**, 171.
23 D. A. McCormack, G. Kroes and D. Neuhauser, *J. Chem. Phys.*, 1998, **109**, 5177.
24 A. García-Vela, *J. Chem. Phys.*, 2002, **116**, 6595.
25 S. Marple, Jr., *Digital Spectral Analysis with Applications*, Prentice-Hall, Englewood Cliffs, NJ, 1987.
26 D. Neuhauser, *J. Chem. Phys.*, 1991, **95**, 4927.
27 M. Alacid and C. Leforestier, *Int. J. Quantum Chem.*, 1998, **68**, 317.
28 M. H. Alexander, G. Capecchi and H. Werner, *Science*, 2002, **296**, 715.
29 R. S. Friedman, T. C. Allison and D. G. Truhlar, *Phys. Chem. Chem. Phys.*, 1999, **1**, 1237.
30 R. S. Friedman, V. M. Ryaboy and N. Moiseyev, *J. Chem. Phys.*, 1999, **111**, 7187.
31 M. D. Feit, J. A. Fleck, Jr. and A. Steiger, *J. Comput. Phys.*, 1982, **47**, 412.
32 D. Kosloff and R. Kosloff, *J. Comput. Phys.*, 1983, **52**, 35.
33 G. Lanczos, *J. Res. Natl. Bur. Stand.*, 1950, **45**, 255.
34 T. J. Park and J. C. Light, *J. Chem. Phys.*, 1986, **85**, 5870.
35 S. Mahapatra and N. Sathyamurhy, *J. Chem. Soc., Faraday Trans.*, 1997, **773**, 93.
36 R. Kosloff and D. Kosloff, *J. Comput. Phys.*, 1986, **63**, 363.
37 F. T. Smith, *Phys. Rev.*, 1960, **118**, 349.
38 F. T. Smith, *J. Chem. Phys.*, 1962, **36**, 248.
39 D. T. Stibbe and J. Tennyson, *Comput. Phys. Commun.*, 1998, **114**, 236.
40 W. H. Press, S. A. Teukolski, W. T. Vetterling, B. P. Flannery, *Numerical Recipes in Fortran: the Art of Scientific Computing*, Cambridge University Press, New York, 1992.

Published on 22 April 2003 on http://pubs.rsc.org | doi:10.1039/B301010D
Downloaded on 15 December 2011